Highly Efficient UV−Violet Light-Emitting Polymers Derived from Fluorene and Tetraphenylsilane Derivatives: Molecular Design toward Enhanced Electroluminescent Performance

Xing-Hua Zhou, Yu-Hua Niu, Fei Huang, Michelle S. Liu, and Alex K.-Y. Jen*

Department of Materials Science and Engineering, Box 352120, University of Washington, Seattle, Washington 98195-2120

Received January 1, 2007; Revised Manuscript Received March 8, 2007

ABSTRACT: Novel fluorene-based light-emitting polymers (**P1**−**P3**) derived form the copolymerization of 9,9-dihexylfluorene or 9,9-spirobifluorene with tetraphenylsilane derivatives were designed and synthesized by palladium-catalyzed Suzuki coupling reaction. These copolymers were readily soluble in common organic solvents and exhibited high glass transition temperature ($T_g \geq 157$ °C) and thermal stability. The results from photophysical studies showed that these copolymers possess a wide band gap (3.26−3.30 eV), which endows them with pure UV−violet emission in solid states with high photoluminescence (PL) quantum efficiencies. The PL characteristic of these copolymers remained almost unchanged in spite of the modification with tetraphenylsilane or even with the electron-donating alkoxyl substituents. The incorporation of bulky 9,9-spirobifluorene units into one of the copolymers (**P3**) significantly improved the solid-state PL quantum efficiency up to 83% together with a slightly red-shifted emission. The LEDs based on **P1**−**P3** exhibited pure UV−violet electroluminescence (EL) emission peaking at 396, 398, and 409 nm, respectively. In comparison with that of **P1**, the devices using **P2** and **P3** exhibited significantly enhanced performance, which was attributed to their higher PL efficiencies and more balanced carriers injection due to the reduced energy barrier for hole injection. A maximum external quantum efficiency of 2.4% and a maximum luminance of 850 cd/m^2 as well as a low turn-on voltage of 5.0 V were demonstrated for **P3**.

Introduction

Organic and polymeric light-emitting devices (OLEDs/PLEDs) have been the subject of intense academic and industrial research in recent years due to their potential applications in large area flat panel displays and general lighting.[1,2] Advances made in the molecular design and synthetic methodologies of high-performance organic optoelectronic materials have contributed to the progress toward the realization of full-color OLEDs displays.[3] One of the remaining challenges in achieving high-quality displays is to develop wide-band-gap materials for achieving highly efficient and stable blue emission. Compared with the considerable efforts devoted to the development of blue-emitting materials, extension of electroluminescent (EL) range into the UV wavelength has not progressed as well even although compact and efficient UV emitters can be utilized to generate emission over the whole visible range and white light emission either by the irradiation of luminescent dyes or via energy transfer to luminescent dopants including emissive phosphors.

Design of amorphous organic materials capable of giving efficient UV emission in OLEDs is quite challenging, especially for luminescent polymers. Among the existing reports of UV-blue-emitting polymers so far, several studies are based on poly(*N*-vinylcarbazole) (PVK)[4] and nonconjugated polymers with luminescent functional groups in the side chains.[5] A class of σ-conjugated polysilanes was also investigated as near-UV-emitting materials for LEDs.[6] Ma et al.[7] reported in 2003 a wide-band-gap conjugated polymer consisting of alternating dihexylfluorene and rigidly twisted biphenyl units and demonstrated its UV electroluminescence peaking at 395 nm. By utilizing a similar copolymerization strategy, a series of blue-violet-emitting poly(fluorene-*co*-thiophene)s have also been developed through the incorporation of various contents of molecularly kinked 3,4-linked thiophene unit into the polyfluorene backbone.[8] Most recently, an UV-emitting conjugated homopolymer, poly(9,9-alkyl-3,6-silafluorene), has been reported to be able to function as a host for green electrophosphorescent emitters due to its sufficiently high triplet energy.[9] However, all the reported EL devices using these materials usually exhibit quite low performance with high turn-on voltages, low quantum efficiencies, and low luminances.[4,6−8]

In our latest communication, we have reported an efficient UV PLED based on an alternating copolymer, poly[2,7-(9,9-dihexylfluorene)-*alt*-4,4′-phenyl ether], with its EL emission peaking at 397 nm and a maximum external quantum efficiency of 1.07%.[10] Xu and He[11] have recently employed a class of tetrahedral precursors of tetraarylsilane to serve as building blocks for constructing efficient and nonaggregating amorphous luminescent materials. Here, we present the rational design, synthesis, and characterization of two fluorene-based alternating copolymers (**P2** and **P3**) derived from 9,9-dihexylfluorene or 9,9-spirobifluorene and novel tetraphenylsilane derivatives (**M2** and **M3**). A related polymer **P1** was also synthesized for comparison in order to systematically investigate their structure−property relationships. This class of copolymers was designed on the basis of the following structural considerations: (i) ability to properly control extended π-conjugation through the δ-Si interrupted structures to achieve UV−violet emission; (ii) use of the twisted polymer backbones and three-dimensional (3D) hindered structures to alleviate the self-aggregation of polymer chains; and (iii) modification of both the fluorene and tetraphenylsilane units to tune the optoelectronic properties for enhanced EL performance. The thermal, optical, and electrochemical properties of **P1**−**P3** were thoroughly investigated in a com-

* Corresponding author. E-mail: ajen@u.washington.edu.

10.1021/ma070003x CCC: $37.00
Published on Web 03/31/2007

Scheme 1. Chemical Structures and Synthetic Approach for the Polymers P1−P3[a]

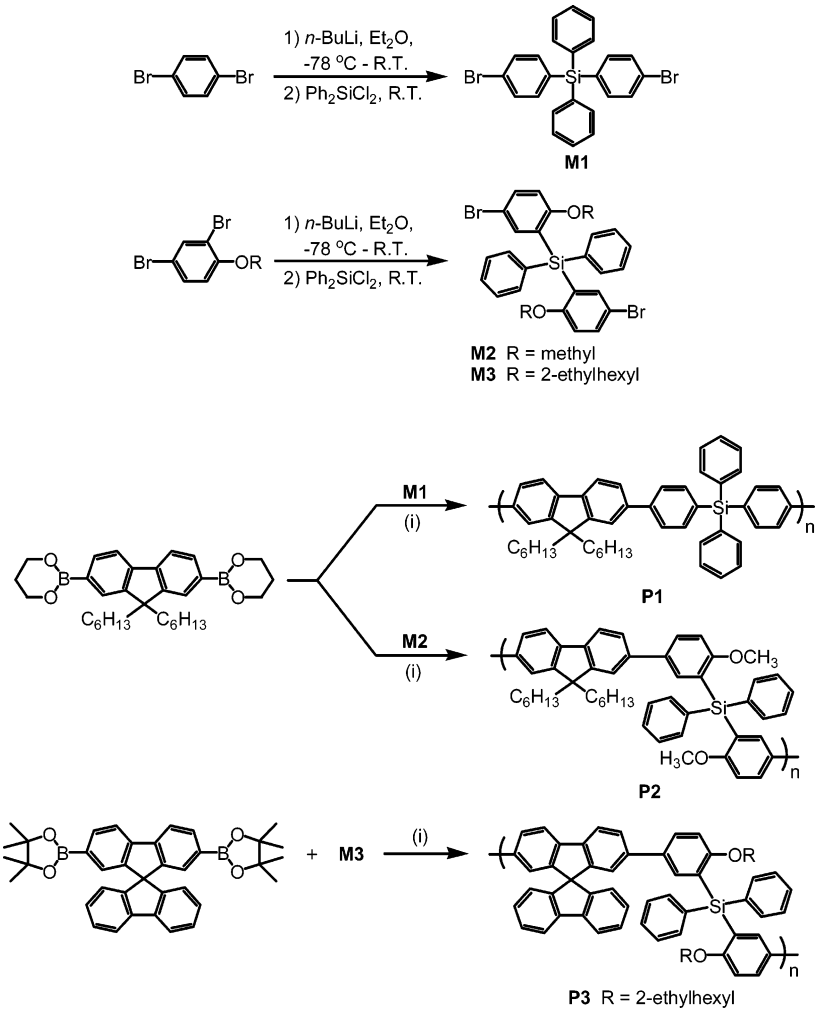

[a] (i) $Pd(PPh_3)_4$, 2 M Na_2CO_3, toluene, 90 °C.

prehensive study. Highly efficient pure UV−violet-emitting PLEDs were fabricated by employing **P2** and **P3** as the emissive layers, both of which exhibited significantly enhanced EL performances in comparison with that of **P1**.

Results and Discussion

The chemical structures and synthetic approach for the polymers **P1**−**P3** are illustrated in Scheme 1. The diboronate monomers, 9,9-dihexylfluorene-2,7-bis(trimethylene boronate)[12] and 2,7-bis(4,4,5,5-tetramethyl-1,3,2-dioxaborolan-2-yl)-9,9-spirobifluorene,[13] were prepared from the corresponding dibromide following the literature procedures, respectively. The synthesis of the key tetraphenylsilane dibromides **M1**−**M3** was achieved by monolithiation of 1,4-dibromobenzene or 2,4-dibromo-1-alkyloxybenzene selectively on the ortho position of alkoxyl groups with *n*-BuLi at −78 °C in diethyl ether and subsequent substitution between the monolithiate and Ph_2SiCl_2, respectively. The palladium-catalyzed Suzuki coupling polymerization was employed to produce the desired polymers in moderate to good yields. The structures of all the tetraphenylsilane derivatives and the resultant polymers were confirmed by ^1H and ^{13}C NMR spectroscopy as well as MS spectroscopy. All three copolymers were readily soluble in common organic solvents such as chloroform, THF, and toluene. The number-average molecular weights (M_n) of **P1**−**P3**, determined by gel permeation chromatography (GPC) using THF as the eluent and polystyrene as standards, were 21 080, 10 790, and 7075, respectively, with a polydispersity index in the range 1.81−2.28.

The thermal properties of **P1**−**P3** were evaluated by thermogravimetric analysis (TGA) and differential scanning calorimetry (DSC) under a nitrogen atmosphere. All materials exhibited an onset of decomposition >400 °C with no weight loss at lower temperature, suggesting their outstanding thermal stability. After thermal annealing upon the first heating to 300 °C, only glass transitions could be observed with no crystallization and melting peak upon further heating beyond the glass transition temperature (T_g), as shown in Figure 1. In comparison with **P1**, **P2** and **P3** showed glass transitions at lower temperature of 157 and 190 °C; however, it is still evident that the incorporation of rigid 9,9-spirobifluorene units into the polymer backbone of **P3** increased the chain rigidity and resulted in a much higher T_g compared to **P2** with 9,9-dihexylfluorene units.

The normalized absorption and photoluminescence (PL) emission spectra of **P1**−**P3** in dilute THF solutions (10^{-6} M) are shown in Figure 2. **P1**, **P2**, and **P3** exhibited similar absorption spectra patterns with the absorption maximum (λ_{max}) at 338, 340, and 342 nm, respectively. Their absorption peaks were considerably blue-shifted relative to those of poly(fluorene-*co*-*alt*-phenylene) derivatives[14] and quite close to that of 2,7-bis(4-methoxylphenyl)-9,9-dihexylfluorene (334 nm),[15] indicating the successful confinement of the effective conjugating lengths due to the δ-Si interrupted polymer backbone. Moreover,

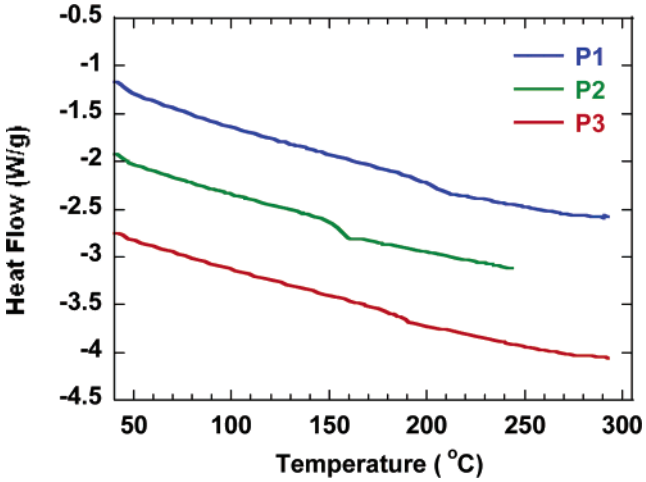

Figure 1. Second heating DSC curves of **P1**−**P3** with a heating rate of 10 °C/min in nitrogen.

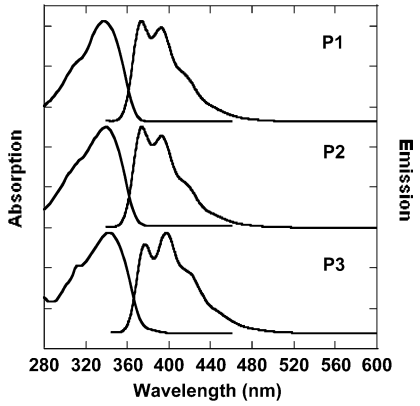

Figure 2. Normalized absorption and PL emission spectra of **P1**−**P3** in THF solutions (10^{-6} M) at room temperature.

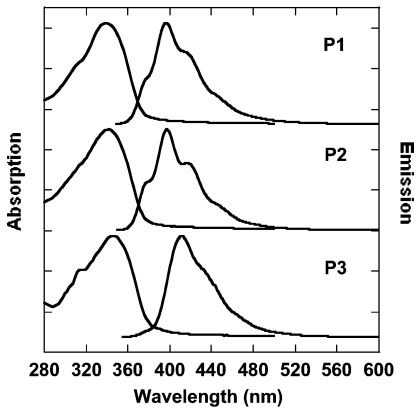

Figure 3. Normalized absorption and PL emission spectra of **P1**−**P3** in solid states at room temperature.

all three polymers displayed a well-defined vibronic structure in their PL spectra, which also indicated that these polymers had a rigid and well-defined backbone structure. **P1** and **P2** exhibited almost the same PL spectra with two vibronic peaks at ca. 374 and 392 nm and a shoulder at ca. 414 nm, while a slight red shift (ca. 3−6 nm) and a little change of the relative intensity were observed for those of **P3** at ca. 377, 398, and 420 nm. Figure 3 shows the absorption and PL emission spectra of **P1**−**P3** in films spin-coated from toluene solutions. The absorption spectra of **P1**−**P3** in films were very similar to those in solutions with only a slight red shift. The optical band gap (E_g) of **P1**−**P3** was in the range 3.26−3.30 eV estimated from

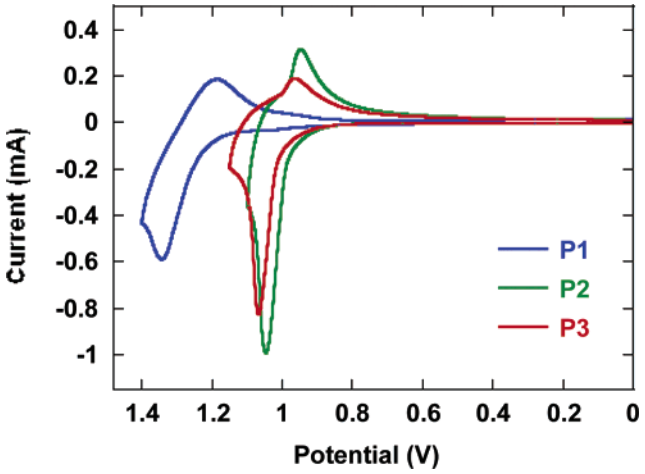

Figure 4. Cyclic voltammograms of **P1**−**P3** films on ITO glass in 0.1 M Bu_4NPF_6 acetonitrile solution at room temperature. The potentials were measured relative to the Ag/Ag^+ reference electrode.

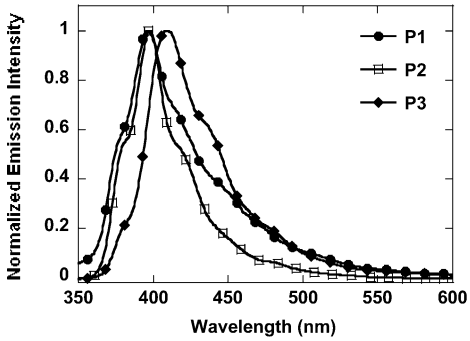

Figure 5. EL spectra of **P1**−**P3** from ITO/PEDOT/polymer/TPBI/CsF/Al devices.

their respective onset wavelengths of film absorption spectra. The PL spectra of all three polymers in films were also red-shifted with respect to the corresponding spectrum in solutions, most obviously for **P3** with a value of 13 nm. Thin films of **P1** and **P2** exhibited intense UV emission with quite similar PL spectra displaying a prominent peak at ca. 396 nm and two shoulders at ca. 378 and 417 nm, respectively. The PL quantum efficiency (Φ_{PL}) was slightly increased from 47% for **P1** to 56% for **P2**. **P3** showed strong violet emission with a peaking at 411 nm and a shoulder at ca. 432 nm, which was red-shifted by about 15 nm from those of **P1** and **P2**. The Φ_{PL} of **P3** films was also significantly improved to 83% due to the effectiveness of the sterically bulky 9,9-spirobifluorene moieties and branched 2-ethylhexyl substituents in blocking the quenching processes associated with intermolecular interactions.

It was noteworthy that the modification of the tetraphenylsilane units on the **P1** and **P2** polymer backbone almost had no effect on their absorption and emission spectra, especially the UV emission characteristic remained intact without obvious shift toward longer wavelengths. However, a red shift (ca. 14 nm) of the thin-film PL spectrum of **P3** was observed in comparison with that of **P2** with the similar backbone structure. Such spectral behaviors were also observed in a series of fluorene-based blue-light-emitting small molecule materials bearing different pendent substituents on the fluorene units.[16] Table 1 summarizes the molecular weights and thermal and optical properties of all three polymers.

To determine the HOMO and LUMO energy levels of **P1**−**P3**, cyclic voltammetry (CV) experiments were conducted in an electrolyte of 0.1 M tetrabutylammonium hexafluorophos-

Table 1. Physical Properties of Polymers P1−P3

			solution λ_{max} (nm)			film λ_{max} (nm)			
compd	M_n (PD)	T_g (°C)	abs	PL	Φ_{PL}[a]	abs	PL	Φ_{PL}[a]	E_g (eV)[b]
P1	21080 (2.28)	204	338	374, 392 (414)	0.80	340	396 (378, 417)	0.47	3.30
P2	10790 (1.84)	157	340	374, 393 (415)	0.92	342	397 (379, 418)	0.56	3.30
P3	7075 (1.81)	190	342	377, 398 (420)	0.99	346	411 (432)	0.83	3.26

[a] The relative photoluminescence quantum efficiencies (Φ_{PL}) of polymers in toluene were determined using a 10^{-5} M solution of 9,10-diphenylanthracene as a standard ($\Phi_{PL} = 93\%$). The Φ_{PL} values of polymer films were determined using 9,10-diphenylanthracene dispersed in PMMA films with a concentration of 10^{-3} M and a quantum efficiency of 83% as a standard. [b] E_g stands for the band-gap energy estimated from their respective onset wavelengths of the optical absorption in films.

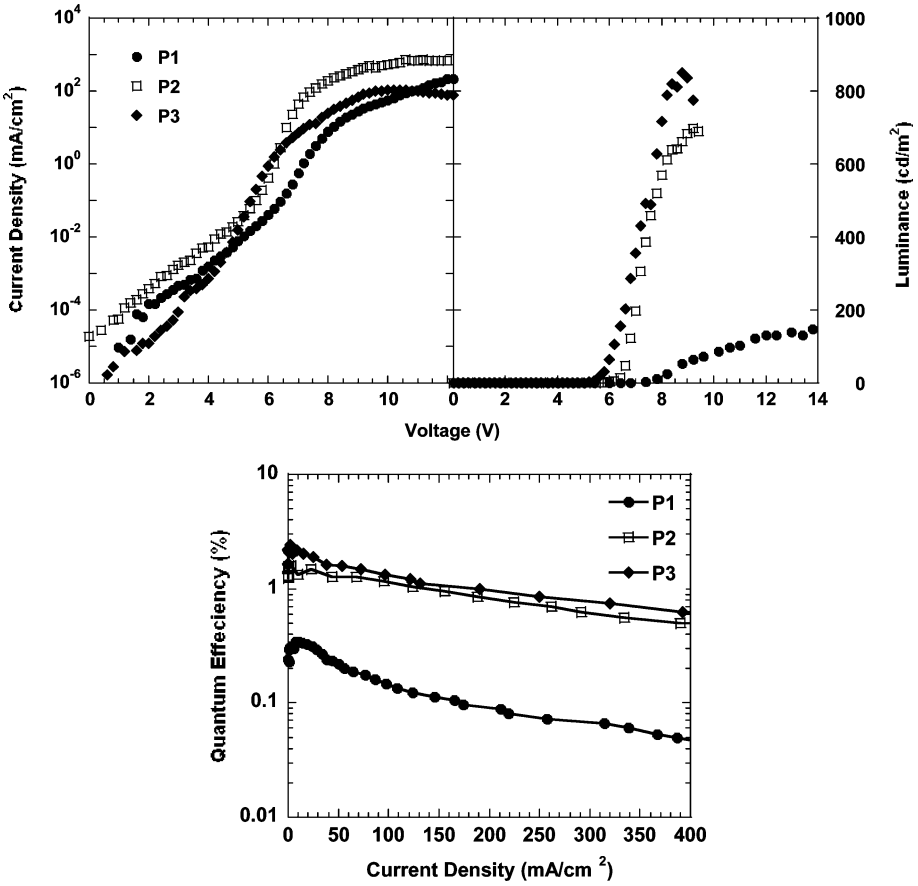

Figure 6. Top: current−voltage ($I-V$) and luminance−voltage ($L-V$) characteristics of ITO/PEDOT/polymer/TPBI/CsF/Al devices. Bottom: external EL quantum efficiency vs current characteristics of the top devices.

phate (TBAPF) in acetonitrile at room temperature under nitrogen with a scan rate of 100 mV/s. The polymers were spin-coated onto the ITO glass and used as the working electrode. The CV curves were referenced to an Ag/Ag^+ reference electrode, which was calibrated using the ferrocene/ferrocenium (Fc/Fc^+) redox couple as the internal standard. As shown in Figure 4, **P1**−**P3** all exhibited a reversible oxidation wave with an onset potential at about 1.11, 0.86, and 0.86 eV, respectively. The onset oxidation potentials of **P2** and **P3** decreased by ca. 0.25 eV in comparison with that of **P1**, which could be attributed to the strong electron-donating feature of the alkoxyl groups in the phenyl rings. The HOMO levels of the polymers were calculated from their corresponding onset oxidation potentials and by assuming the energy level of Fc/Fc^+ to be 4.8 eV below the vacuum level ($E_{Fc}^{onset} = -0.07$ V vs Ag/Ag^+).[17] The HOMO levels of both **P2** and **P3** were noticeably raised from −5.98 eV for **P1** to −5.73 eV, which implied a significant lowering of the energy barrier for hole injecting from ITO anode. Unfortunately, we were unable to record the reduction process of the polymers and the corresponding LUMO level of **P1**−**P3** could only be estimated from the HOMO level and optical band gap.

To investigate their EL properties, the LEDs with **P1**−**P3** as the emitting layers were fabricated with the configuration of ITO/PEDOT:PSS/polymers/TPBI/CsF/Al, where a conducting polymer, poly(3,4-ethylene dioxythiophene) (PEDOT), doped with poly(styrenesulfonic acid) (PSS) was used as the hole-injection layer, and a small molecule compound, 2,2′,2″-(1,3,5-benzenetriyl)tris[1-phenyl-1*H*-benzimidazole] (TPBI), was used as the electron-transporting/hole-blocking layer, and 10 Å CsF was used with Al as the electron-injection layer. As shown in Figure 5, structured EL in the UV−violet region was achieved from these devices with an emission peak at 396, 398, and 409 nm and a narrow fwhm (full width at half-maximum) of 41−54 nm, which matched well with their corresponding solid-state PL emissions. Moreover, the EL spectra of these devices exhibited no obvious voltage dependence below 10 V, only with a slightly increase on the long wavelength at ca. 476 nm, and no obvious emission in the range of 500−600 nm was observed. Such EL spectra features is advantageous for this series of

Table 2. Electroluminescent Device Performances of P1−P3

compd	λ_{max}^{EL}/ fwhm (nm)	V_{on} (V)	η_{ext} (%, 100 cd m^{-2})	$\eta_{max,ext}$ (%)	L_{max} (cd m^{-2}, V)
P1	396/54	7.0	0.15	0.34	152, 13.6
P2	398/41	5.8	1.49	1.59	696, 9.4
P3	409/51	5.0	2.04	2.40	850, 8.8

fluorene-based luminescent copolymers with such short-wavelength emissions because a large fraction of polyfluorene-type blue-light-emitting polymers often suffer from their tendency to form π-aggregates/excimers or ketonic defects during passage of current, leading to a red-shifted green emission.[18] Considering the structure characteristics of **P1**−**P3**, the improved color purity and stability were attributed to their twisted and δ-Si conjugation interrupted polymer backbones as well as the 3D sterically hindered structures (especially for **P2** and **P3**). This not only significantly reduced the self-aggregation of polymer chains but also hindered the undesired exciton energy transfer to some potential structural defects due to the quantum confinement effect.[11f]

The current−voltage ($I-V$) and luminance−voltage ($L-V$) characteristics as well as the external quantum efficiency as a function of current for the EL devices based on **P1**−**P3** are shown in Figure 6. In comparison with that of **P1**, the devices from **P2** and **P3** exhibited greatly enhanced performance in terms of turn-on voltage, luminance, and external quantum efficiency. For example, the devices of **P2** and **P3** showed much lower turn-on voltages of 5.8 and 5.0 V (defined as the voltage required to give a luminance of 1 cd/m^2), respectively, and rather low driving voltage regardless of their intrinsic wide band gaps. The device based on **P2** showed a maximum external quantum efficiency of 1.59% and a maximum luminance of 696 cd/m^2, which were more than 4 times higher than those of the device from **P1** with the identical UV emission characteristics. For the **P3**-based device, its maximum external quantum efficiency further increased to 2.4% with an even higher maximum luminance of 850 cd/m^2 although its EL emission was slightly red-shifted into the blue region. The significantly enhanced device performances of **P2** and **P3** were considered to be the result from their higher PL efficiencies and more efficient and balanced carriers injection due to the lowered energy barrier for hole injection. To the best of our knowledge, the performances of the devices based on **P2** and **P3** are among the highest for such short-wavelength PLEDs in the UV−violet region employing the neat emissive layer. The characteristics of all three EL devices are summarized in Table 2.

Conclusion

A series of fluorene-based light-emitting polymers (**P1**−**P3**) derived form the copolymerization of 9,9-dihexylfluorene or 9,9-spirobifluorene with tetraphenylsilane derivatives were designed and synthesized by palladium-catalyzed Suzuki coupling reaction. These copolymers were readily soluble in common organic solvents and exhibited high glass transition temperature ($T_g \geq$ 157 °C) and thermal stability. The results from photophysical studies showed that these copolymers possess a wide band gap (3.26−3.30 eV) which endows them with pure UV−violet emission in solid states with high photoluminescence (PL) quantum efficiencies. The PL characteristic of these copolymers remained almost unchanged in spite of the modification with tetraphenylsilane or even with the electron-donating alkoxyl substituents. The incorporation of bulky 9,9-spirobifluorene units into one of the copolymers (**P3**) significantly improved the solid-state PL quantum efficiency up to 83% together with a slightly red-shifted emission. The LEDs based on **P1**−**P3** exhibited pure UV−violet electroluminescence (EL) emission peaking at 396, 398, and 409 nm, respectively. In comparison with that of **P1**, the devices using **P2** and **P3** exhibited significantly enhanced performance, which was attributed to their higher PL efficiencies and more balanced carriers injection due to the reduced energy barrier for hole injection. A maximum external quantum efficiency of 2.4% and a maximum luminance of 850 cd/m^2 as well as a low turn-on voltage of 5.0 V were demonstrated for **P3**.

Experimental Section

General Methods. Chemicals were purchased from Aldrich and used as received. ^{1}H and ^{13}C NMR spectra were recorded on a Bruker AV300 and AV500 spectrometer using $CDCl_3$ as solvent in all cases. EI-MS and ESI-MS spectra were recorded on a JEOL HX-110 and Bruker APEX III 47e Fourier transform mass spectrometer, respectively. Molecular weights of the polymers were determined by a Waters 1515 gel permeation chromatograph (GPC) with a refractive index detector in tetrahydrofuran using a calibration curve of polystyrene standards. Thermal properties of the polymers were analyzed with a TA Instruments thermal analysis and rheology system (TGA 2950, DSC 2010) under nitrogen at a heating rate of 10 °C/min. Cyclic voltametric data were measured on a BAS CV-50W voltametric analyzer using tetrabutylammonium hexafluorophosphate (0.1 M) in acetonitrile (electrochemical grade, Fisher Scientific) as electrolyte and indium tin oxide (ITO) and Ag/Ag$^+$ as the working and reference electrode, respectively. UV−vis spectra were recorded on a Perkin-Elmer spectrophotometer (Lambda 9 UV/vis/NIR). PL spectra were carried out on Perkin-Elmer LS 50B luminescence spectrometer. The relative photoluminescence quantum efficiencies (Φ_{PL}) of polymers in toluene were determined using a 10^{-5} M solution of 9,10-diphenylanthracene as a standard (Φ_{PL} = 93%). The Φ_{PL} values of polymer films were determined using 9,10-diphenylanthracene dispersed in PMMA films with a concentration of 10^{-3} M and a quantum efficiency of 83% as a standard. EL spectra were recorded by the Oriel Instaspec IV spectrometer with a CCD detector. Current−voltage ($I-V$) and luminance−voltage ($L-V$) characteristics were measured on a Hewlett-Packard 4155B semiconductor parameter analyzer together with a Newport 2835-C multifunctional optical meter. Photometric units (cd/m^2) were calculated using the forward output power and the EL spectra of the devices, assuming Lambertian distribution of the EL emission.

EL Device Fabrication. The LEDs were fabricated on indium tin oxide (ITO)-coated glass substrates with sheet resistance 20 Ω/sq. The substrate was ultrasonic cleaned with acetone, detergent, deionized water, and 2-propanol. Oxygen plasma treatment was made for 10 min as the final step of substrate cleaning to improve the contact angle just before film coating. Onto the ITO glass was spin-coated a layer of PEDOT:PSS film with thickness of 50 nm from its aqueous dispersion, aiming to improve the hole injection and to avoid the possibility of leakage. PEDOT:PSS film was dried at 80 °C for 2 h in the vacuum oven. The solution of the polymer in toluene was prepared in a nitrogen-filled drybox and spin-coated on top of the ITO/PEDOT:PSS surface. Measured by a Sloan Dektak 3030 surface profiler, the typical thickness of the emitting layer was 40−60 nm. In a vacuum below 1×10^{-6} Torr, 1,3,5-tris(*N*-phenylbenzimidazol-2-yl)benzene (TPBI, 25 nm) was sublimed. Cesium fluoride with thickness of 1 nm and aluminum of 200 nm were evaporated subsequently as cathode. The active emissive area defined by the cathode was about 3 mm^2. All device testing was carried out in air at room temperature.

Compound M1. 1,4-Dibromobenzene (2.95 g, 12.5 mmol) was dissolved in dry diethyl ether and cooled to −78 °C in an acetone/dry ice bath. To the solution was added *n*-BuLi (2.5 M, 5.5 mL, 1.1 equiv) dropwise via a syringe. Then the acetone/dry ice bath was removed, and the solution was stirred for 1 h at room temperature. The solution was cooled down to −78 °C again and then was added dichlorodiphenylsilane (1.26 g, 5.0 mmol) in one portion. The reaction mixture was slowly warmed to room

temperature and stirred overnight. Upon completion, the reaction mixture was poured into water and extracted with ethyl acetate. The combined organic solution was washed with brine and dried over $MgSO_4$. The crude product was purified by column chromatography (hexanes/dichloromethane) to give the product as a white solid in 65% yield (1.61 g). ^{1}H NMR ($CDCl_3$, 300 MHz, ppm): 7.55−7.35 (18H, m, Ar−H). ^{13}C NMR ($CDCl_3$, 125 MHz, ppm): 137.81, 136.21, 132.98, 132.63, 131.21, 130.00, 128.09, 124.96. EI-MS (*m*/*e*): 494.5 (M^+).

Compound M2. The procedure for **M1** was followed to prepare **M2** from 2,4-dibromoanisole (4.86 g, 18.3 mmol) and dichlorodiphenylsilane (2.00 g, 7.9 mmol) as a white solid in 63% yield (2.77 g). ^{1}H NMR ($CDCl_3$, 300 MHz, ppm): 7.53−7.47 (6H, m, Ar−H), 7.41−7.25 (8H, m, Ar−H), 6.78−6.75 (2H, d, J = 8.7 Hz, Ar−H), 3.45 (6H, s, OCH_3). ^{13}C NMR ($CDCl_3$, 125 MHz, ppm): 163.24, 140.07, 135.90, 134.19, 134.03, 129.16, 127.49, 126.20, 113.62, 112.41, 55.28. ESI-MS (*m*/*e*): 576.9613 ($M + Na^+$).

Compound M3. The procedure for **M1** was followed to prepare **M3** from 2,4-dibromo-1-(2′-ethylhexoxy)benzene (5.10 g, 14.0 mmol) and dichlorodiphenylsilane (1.60 g, 6.3 mmol) as a white solid in 38% yield (1.78 g). ^{1}H NMR ($CDCl_3$, 300 MHz, ppm): 7.48−7.43 (6H, m, Ar−H), 7.38−7.22 (8H, m, Ar−H), 6.77−6.74 (2H, d, J = 8.7 Hz, Ar−H), 3.59−3.56 (4H, m, OCH_2), 1.11−0.91 (10H, m, CH, CH_2), 0.86−0.73 (14H, m, CH_2, CH_3), 0.59−0.54 (6H, t, J = 7.2 Hz, CH_3). ^{13}C NMR ($CDCl_3$, 125 MHz, ppm): 162.84, 140.35, 135.95, 134.06, 133.99, 129.15, 127.50, 125.93, 113.15, 112.11, 70.20, 38.91, 29.83, 28.98, 22.85, 22.74, 14.07, 10.90. ESI-MS (*m*/*e*): 789.1574 ($M + K^+$).

Polymer P1. 9,9-Dihexylfluorene-2,7-bis(trimethylene boronate) (377 mg, 0.75 mmol), compound **M1** (371 mg, 0.75 mmol), and 1.5 mol % $Pd(PPh_3)_4$ were dissolved in toluene (5 mL) and 2 M aqueous sodium carbonate solution (3 mL). The reaction mixture was degassed by bubbling with N_2 and then was vigorously stirred at 90−100 °C for 2 days. At the end of polymerization, 9,9-dihexylfluorene-2,7-bis(trimethylene boronate) and bromobenzene were added sequentially for end-capping. The mixture was poured into stirred 100 mL of methanol to precipitate plenty of solids. The solid was collected by filtration and washed with methanol and water. The residue was dissolved in THF and dedoped by stirring in $NH_2NH_2 \cdot H_2O$ for 24 h. The organic layer was isolated, and the concentrated solution was added dropwise into methanol to precipitate the polymer. The solids were isolated by filtration and washed with methanol again. The polymer was further purified by washing with refluxing acetone in Soxhlet for 2 days and was dried under vacuum at room temperature to afford the desired polymer as a white solid in 72% (360 mg). ^{1}H NMR ($CDCl_3$, 300 MHz, ppm): 7.79−7.60 (18H, m, Ar−H), 7.49−7.39 (6H, m, Ar−H), 2.03−2.00 (4H, m, CH_2), 1.13−1.05 (12H, m, CH_2), 0.76−0.71 (10H, m, CH_2, CH_3). ^{13}C NMR ($CDCl_3$, 125 MHz, ppm): 151.73, 142.68, 140.29, 139.73, 136.93, 136.41, 134.23, 132.81, 129.68, 127.95, 126.61, 126.08, 121.48, 120.10, 55.26, 40.50, 31.45, 29.71, 23.81, 22.55, 13.96.

Polymer P2. The procedure for **P1** was followed to produce **P2** using 9,9-dihexylfluorene-2,7-bis(trimethylene boronate) and compound **M2** as a white solid in 55% yield. ^{1}H NMR ($CDCl_3$, 300 MHz, ppm): 7.72−7.66 (6H, m, Ar−H), 7.60−7.58 (4H, m, Ar−H), 7.40−7.29 (10H, m, Ar−H), 7.03−7.00 (2H, d, J = 8.4 Hz, Ar−H), 3.61 (6H, s, OCH_3), 1.87−1.85 (4H, m, CH_2), 1.08−0.95 (12H, m, CH_2), 0.71−0.66 (6H, t, J = 7.2 Hz, CH_3), 0.53 (4H, br, CH_2). ^{13}C NMR ($CDCl_3$, 125 MHz, ppm): 164.01, 151.26, 139.50, 139.41, 137.32, 136.13, 135.51, 133.74, 129.98, 128.90, 127.31, 125.19, 123.58, 120.74, 119.64, 110.48, 55.22, 54.97, 40.77, 31.46, 29.89, 23.71, 22.60, 13.97.

Polymer P3. The procedure for **P1** was followed to produce **P3** using 2,7-bis(4,4,5,5-tetramethyl-1,3,2-dioxaborolan-2-yl)-9,9-spirobifluorene and compound **M3** as a white solid in 43% yield. ^{1}H NMR ($CDCl_3$, 300 MHz, ppm): 7.81−7.78 (2H, d, J = 7.5 Hz, Ar−H), 7.71−7.68 (2H, d, J = 8.1 Hz, Ar−H), 7.41−7.32 (8H, m, Ar−H), 7.24−7.19 (4H, m, Ar−H), 7.13−7.08 (6H, m, Ar−H), 6.95−6.90 (2H, t, J = 7.2 Hz, Ar−H), 6.67−6.57 (6H, m, Ar−H), 3.34 (4H, br, OCH_2), 0.90−0.76 (10H, m, CH, CH_2), 0.65−0.52 (14H, m, CH_2, CH_3), 0.39−0.35 (6H, t, J = 7.2 Hz, CH_3). ^{13}C NMR ($CDCl_3$, 125 MHz, ppm): 163.41, 149.33, 148.95, 141.64, 140.19, 139.80, 137.00, 135.78, 135.15, 131.93, 129.44, 128.62, 127.89, 127.60, 127.06, 125.72, 124.49, 121.69, 119.84, 119.58, 109.90, 69.48, 65.88, 53.40, 39.00, 29.78, 28.96, 22.62, 13.99, 10.98.

Acknowledgment. Financial support from the National Science Foundation (the NSF-STC Program under Agreement DMR-0120967) and the Air Force Office of Scientific Research (AFOSR) under the MURI Center on Polymeric Smart Skins is acknowledged. Alex. K.-Y. Jen thanks the Boeing-Johnson Foundation for its support.

References and Notes

(1) Tang, C. W.; VanSlyke, S. A. *Appl. Phys. Lett.* **1987**, *51*, 913.

(2) Burroughes, J. H.; Bradley, D. D. C.; Brown, A. R.; Marks, R. N.; Mackay, K.; Friend, R. H.; Burns, P. L.; Holmes, A. B. *Nature (London)* **1990**, *347*, 539.

(3) (a) Kraft, A.; Grimsdale, A. C.; A. C.; Holmes, A. B. *Angew. Chem., Int. Ed.* **1998**, *37*, 927. (b) Mitschke, U.; Bäuerle, P. *J. Mater. Chem.* **2000**, *10*, 1471. (c) Bernius, M. T.; Inbasekaran, M.; O'Brien, J.; Wu, W. *Adv. Mater.* **2000**, *12*, 1737. (d) Akcelrud, L. *Prog. Polym. Sci.* **2003**, *28*, 875.

(4) Kido, J.; Hongawa, K.; Okuyama, K.; Nagai, K. *Appl. Phys. Lett.* **1993**, *63*, 2627.

(5) (a) Fehervari, A. F.; Kagumba, L. C.; Hadjikyriacou, S.; Chen, F.; Gaudiana, R. A. *J. Appl. Polym. Sci.* **2003**, *87*, 1634. (b) Spiliopoulos, L. K.; Mikroyannidis, J. A. *Macromolecules* **2002**, *35*, 7254.

(6) (a) Yuan, C. H.; Hoshino, S.; Toyoda, S.; Suzuki, H.; Fujiki, M.; Matsumoto, N. *Appl. Phys. Lett.* **1997**, *71*, 3326. (b) Hoshino, S.; Ebata, K.; Furukawa, K. *J. Appl. Phys.* **2000**, *87*, 1968.

(7) Lu, P.; Zhang, H.; Shen, F.; Yang, B.; Li, D.; Ma, Y.; Chen, X.; Li, J.; Tamai, N. *Macromol. Chem. Phys.* **2003**, *204*, 2274.

(8) Vamvounis, G.; Schulz, G. L.; Holdcroft, S. *Macromolecules* **2004**, *37*, 8897.

(9) (a) Mo, Y. Q.; Tian, R. Y.; Shi, W.; Cao, Y. *Chem. Commun.* **2005**, *39*, 4925. (b) Chan, K. L.; Watkins, S. E.; Mak, C. S. K.; McKiernan, M. J.; Towns, C. R.; Pascu, S. I.; Holmes, A. B. *Chem. Commun.* **2005**, *39*, 5766.

(10) Huang, F.; Niu, Y.-H.; Liu, M. S.; Zhou, X.-H.; Tian, Y.-Q.; Jen, A. K.-Y. *Appl. Phys. Lett.* **2006**, *89*, 081104.

(11) (a) Liu, X.-M.; He, C.; Hao, X.-T.; Tan, L.-W.; Li, Y.; Ong, K. S. *Macromolecules* **2004**, *37*, 5965. (b) Liu, X.-M.; He, C.; Huang, J.; Xu, J. *Chem. Mater.* **2005**, *17*, 434. (c) Liu, X.-M.; Lin, T.; Huang, J.; Hao, X.-T.; Ong, K. S.; He, C. *Macromolecules* **2005**, *38*, 4157. (d) Liu, X.-M.; Xu, J.; Lu, X.; He, C. *Org. Lett.* **2005**, *7*, 2829. (f) Liu, X.-M.; Xu, J.; Lu, X.; He, C. *Macromolecules* **2006**, *39*, 1397.

(12) Zhou, X.-H.; Yan, J.-C.; Pei, J. *Macromolecules* **2004**, *37*, 7078.

(13) Wong, K.-T.; Chien, Y.-Y.; Chen, R.-T.; Wang, C.-F.; Lin, Y.-T.; Chiang, H.-H.; Hsieh, P.-Y.; Wu, C.-C.; Chou, C. H.; Su, Y. O.; Lee, G.-H.; Peng, S.-M. *J. Am. Chem. Soc.* **2002**, *124*, 11576.

(14) Liu, B.; Yu, W.-L.; Lai, Y.-H.; Huang, W. *Chem. Mater.* **2001**, *13*, 1984.

(15) Cho, H. N.; Chung, S.-H.; Song, S.-W. Jpn. Kokai Tokkyo Koho JP 2003064003, 2003.

(16) Tan, S.; Peng, Z.; Zhang, X.; Wang, P.; Lee, C.-S.; Lee, S.-T. *Adv. Funct. Mater.* **2005**, *15*, 1716.

(17) Thelakkat, M.; Svhmidt, H.-W. *Adv. Mater.* **1998**, *10*, 219.

(18) (a) Bliznyuk, V. N.; Carter, S. A.; Scott, J. C.; Klärner, G.; Miller, R. D.; Miller, D. C. *Macromolecules* **1999**, *32*, 361. (b) Weinfurtner, K.-H.; Fujikawa, H.; Tokito, S.; Taga, Y. *Appl. Phys. Lett.* **2000**, *76*, 2502. (c) List, E. J. W.; Güntner, R.; Scanducci de Freitas, P.; Scherf, U. *Adv. Mater.* **2002**, *14*, 374. (d) Gong, X.; Iyer, P. K.; Moses, D.; Bazan, G. C.; Heeger, A. J.; Xiao, S. S. *Adv. Funct. Mater.* **2003**, *13*, 325. (e) Zhou, X.-H.; Zhang, Y.; Xie, Y.-Q.; Cao, Y.; Pei, J. *Macromolecules* **2006**, *39*, 3830.

MA070003X